

Observation of the Decay $D^0 \rightarrow \rho^- \mu^+ \nu_\mu$

- M. Ablikim¹, M. N. Achasov^{10,c}, P. Adlarson⁶⁷, S. Ahmed¹⁵, M. Albrecht⁴, R. Aliberti²⁸, A. Amoroso^{66A,66C}, M. R. An³², Q. An^{63,49}, X. H. Bai⁵⁷, Y. Bai⁴⁸, O. Bakina²⁹, R. Baldini Ferroli^{23A}, I. Balossino^{24A}, Y. Ban^{38,k}, K. Begzsuren²⁶, N. Berger²⁸, M. Bertani^{23A}, D. Bettoni^{24A}, F. Bianchi^{66A,66C}, J. Bloms⁶⁰, A. Bortone^{66A,66C}, I. Boyko²⁹, R. A. Briere⁵, H. Cai⁶⁸, X. Cai^{1,49}, A. Calcaterra^{23A}, G. F. Cao^{1,54}, N. Cao^{1,54}, S. A. Cetin^{53A}, J. F. Chang^{1,49}, W. L. Chang^{1,54}, G. Chelkov^{29,b}, D. Y. Chen⁶, G. Chen¹, H. S. Chen^{1,54}, M. L. Chen^{1,49}, S. J. Chen³⁵, X. R. Chen²⁵, Y. B. Chen^{1,49}, Z. J. Chen^{20,l}, W. S. Cheng^{66C}, G. Cibinetto^{24A}, F. Cossio^{66C}, X. F. Cui³⁶, H. L. Dai^{1,49}, X. C. Dai^{1,54}, A. Dbeysi¹⁵, R. E. de Boer⁴, D. Dedovich²⁹, Z. Y. Deng¹, A. Denig²⁸, I. Denysenko²⁹, M. Destefanis^{66A,66C}, F. De Mori^{66A,66C}, Y. Ding³³, C. Dong³⁶, J. Dong^{1,49}, L. Y. Dong^{1,54}, M. Y. Dong^{1,49,54}, X. Dong⁶⁸, S. X. Du⁷¹, Y. L. Fan⁶⁸, J. Fang^{1,49}, S. S. Fang^{1,54}, Y. Fang¹, R. Farinelli^{24A}, L. Fava^{66B,66C}, F. Feldbauer⁴, G. Felici^{23A}, C. Q. Feng^{63,49}, J. H. Feng⁵⁰, M. Fritsch⁴, C. D. Fu¹, Y. Gao^{63,49}, Y. Gao^{38,k}, Y. Gao⁶⁴, Y. G. Gao⁶, I. Garzia^{24A,24B}, P. T. Ge⁶⁸, C. Geng⁵⁰, E. M. Gersabeck⁵⁸, A. Gilman⁶¹, K. Goetzen¹¹, L. Gong³³, W. X. Gong^{1,49}, W. Gradl²⁸, M. Greco^{66A,66C}, L. M. Gu³⁵, M. H. Gu^{1,49}, S. Gu², Y. T. Gu¹³, C. Y. Guan^{1,54}, A. Q. Guo²², L. B. Guo³⁴, R. P. Guo⁴⁰, Y. P. Guo^{9,h}, A. Guskov^{29,b}, T. T. Han⁴¹, W. Y. Han³², X. Q. Hao¹⁶, F. A. Harris⁵⁶, N. Hüskens^{22,28}, K. L. He^{1,54}, F. H. Heinsius⁴, C. H. Heinz²⁸, T. Held⁴, Y. K. Heng^{1,49,54}, C. Herold⁵¹, M. Himmelreich^{11,f}, T. Holtmann⁴, G. Y. Hou^{1,54}, Y. R. Hou⁵⁴, Z. L. Hou¹, H. M. Hu^{1,54}, J. F. Hu^{47,m}, T. Hu^{1,49,54}, Y. Hu¹, G. S. Huang^{63,49}, L. Q. Huang⁶⁴, X. T. Huang⁴¹, Y. P. Huang¹, Z. Huang^{38,k}, T. Hussain⁶⁵, W. Ikegami Andersson⁶⁷, W. Imoehl²², M. Irshad^{63,49}, S. Jaeger⁴, S. Janchiv^{26,j}, Q. Ji¹, Q. P. Ji¹⁶, X. B. Ji^{1,54}, X. L. Ji^{1,49}, Y. Y. Ji⁴¹, H. B. Jiang⁴¹, X. S. Jiang^{1,49,54}, J. B. Jiao⁴¹, Z. Jiao¹⁸, S. Jin³⁵, Y. Jin⁵⁷, M. Q. Jing^{1,54}, T. Johansson⁶⁷, N. Kalantar-Nayestanaki⁵⁵, X. S. Kang³³, R. Kappert⁵⁵, M. Kavatsyuk⁵⁵, B. C. Ke^{43,1}, I. K. Keshk⁴, A. Khoukaz⁶⁰, P. Kiese²⁸, R. Kiuchi¹, R. Kliemt¹¹, L. Koch³⁰, O. B. Kolcu^{53A,e}, B. Kopf⁴, M. Kuemmel⁴, M. Kuessner⁴, A. Kupsc⁶⁷, M. G. Kurth^{1,54}, W. Kühn³⁰, J. J. Lane⁵⁸, J. S. Lange³⁰, P. Larin¹⁵, A. Lavania²¹, L. Lavezzi^{66A,66C}, Z. H. Lei^{63,49}, H. Leithoff²⁸, M. Lellmann²⁸, T. Lenz²⁸, C. Li³⁹, C. H. Li³², Cheng Li^{63,49}, D. M. Li⁷¹, F. Li^{1,49}, G. Li¹, H. Li^{63,49}, H. Li⁴³, H. B. Li^{1,54}, H. J. Li¹⁶, J. L. Li⁴¹, J. Q. Li⁴, J. S. Li⁵⁰, Ke Li¹, L. K. Li¹, Lei Li³, P. R. Li^{31,n,o}, S. Y. Li⁵², W. D. Li^{1,54}, W. G. Li¹, X. H. Li^{63,49}, X. L. Li⁴¹, Xiaoyu Li^{1,54}, Z. Y. Li⁵⁰, H. Liang^{1,54}, H. Liang^{63,49}, H. Liang²⁷, Y. F. Liang⁴⁵, Y. T. Liang²⁵, G. R. Liao¹², L. Z. Liao^{1,54}, J. Libby²¹, C. X. Lin⁵⁰, B. J. Liu¹, C. X. Liu¹, D. Liu^{15,63}, F. H. Liu⁴⁴, Fang Liu¹, Feng Liu⁶, H. B. Liu¹³, H. M. Liu^{1,54}, Huanhuan Liu¹, Huihui Liu¹⁷, J. B. Liu^{63,49}, J. L. Liu⁶⁴, J. Y. Liu^{1,54}, K. Liu¹, K. Y. Liu³³, L. Liu^{63,49}, M. H. Liu^{9,h}, P. L. Liu¹, Q. Liu⁵⁴, Q. Liu⁶⁸, S. B. Liu^{63,49}, Shuai Liu⁴⁶, T. Liu^{1,54}, W. M. Liu^{63,49}, X. Liu^{31,n,o}, Y. Liu^{31,n,o}, Y. B. Liu³⁶, Z. A. Liu^{1,49,54}, Z. Q. Liu⁴¹, X. C. Lou^{1,49,54}, F. X. Lu⁵⁰, H. J. Lu¹⁸, J. D. Lu^{1,54}, J. G. Lu^{1,49}, X. L. Lu¹, Y. Lu¹, Y. P. Lu^{1,49}, C. L. Luo³⁴, M. X. Luo⁷⁰, P. W. Luo⁵⁰, T. Luo^{9,h}, X. L. Luo^{1,49}, X. R. Lyu⁵⁴, F. C. Ma³³, H. L. Ma¹, L. L. Ma⁴¹, M. M. Ma^{1,54}, Q. M. Ma¹, R. Q. Ma^{1,54}, R. T. Ma⁵⁴, X. X. Ma^{1,54}, X. Y. Ma^{1,49}, F. E. Maas¹⁵, M. Maggiora^{66A,66C}, S. Maldaner⁴, S. Malde⁶¹, Q. A. Malik⁶⁵, A. Mangoni^{23B}, Y. J. Mao^{38,k}, Z. P. Mao¹, S. Marcello^{66A,66C}, Z. X. Meng⁵⁷, J. G. Messchendorp⁵⁵, G. Mezzadri^{24A}, T. J. Min³⁵, R. E. Mitchell²², X. H. Mo^{1,49,54}, Y. J. Mo⁶, N. Yu. Muchnoi^{10,c}, H. Muramatsu⁵⁹, S. Nakhoul^{11,f}, Y. Nefedov²⁹, F. Nerling^{11,f}, I. B. Nikolaev^{10,c}, Z. Ning^{1,49}, S. Nisar^{8,i}, S. L. Olsen⁵⁴, Q. Ouyang^{1,49,54}, S. Pacetti^{23B,23C}, X. Pan^{9,h}, Y. Pan⁵⁸, A. Pathak¹, P. Patteri^{23A}, M. Pelizaeus⁴, H. P. Peng^{63,49}, K. Peters^{11,f}, J. Pettersson⁶⁷, J. L. Ping³⁴, R. G. Ping^{1,54}, R. Poling⁵⁹, V. Prasad^{63,49}, H. Qi^{63,49}, H. R. Qi⁵², K. H. Qi²⁵, M. Qi³⁵, T. Y. Qi⁹, S. Qian^{1,49}, W. B. Qian⁵⁴, Z. Qian⁵⁰, C. F. Qiao⁵⁴, L. Q. Qin¹², X. P. Qin⁹, X. S. Qin⁴¹, Z. H. Qin^{1,49}, J. F. Qiu¹, S. Q. Qu³⁶, K. H. Rashid⁶⁵, K. Ravindran²¹, C. F. Redmer²⁸, A. Rivetti^{66C}, V. Rodin⁵⁵, M. Rololo^{66C}, G. Rong^{1,54}, Ch. Rosner¹⁵, M. Rump⁶⁰, H. S. Sang⁶³, A. Sarantsev^{29,d}, Y. Schelhaas²⁸, C. Schnier⁴, K. Schoenning⁶⁷, M. Scodeggio^{24A,24B}, D. C. Shan⁴⁶, W. Shan¹⁹, X. Y. Shan^{63,49}, J. F. Shangguan⁴⁶, M. Shao^{63,49}, C. P. Shen⁹, H. F. Shen^{1,54}, P. X. Shen³⁶, X. Y. Shen^{1,54}, H. C. Shi^{63,49}, R. S. Shi^{1,54}, X. Shi^{1,49}, X. D. Shi^{63,49}, J. J. Song⁴¹, W. M. Song^{27,1}, Y. X. Song^{38,k}, S. Sosio^{66A,66C}, S. Spataro^{66A,66C}, K. X. Su⁶⁸, P. P. Su⁴⁶, F. F. Sui⁴¹, G. X. Sun¹, H. K. Sun¹, J. F. Sun¹⁶, L. Sun⁶⁸, S. S. Sun^{1,54}, T. Sun^{1,54}, W. Y. Sun²⁷, W. Y. Sun³⁴, X. Sun^{20,l}, Y. J. Sun^{63,49}, Y. K. Sun^{63,49}, Y. Z. Sun¹, Z. T. Sun¹, Y. H. Tan⁶⁸, Y. X. Tan^{63,49}, C. J. Tang⁴⁵, G. Y. Tang¹, J. Tang⁵⁰, J. X. Teng^{63,49}, V. Thoren⁶⁷, W. H. Tian⁴³, Y. T. Tian²⁵, I. Uman^{53B}, B. Wang¹, C. W. Wang³⁵, D. Y. Wang^{38,k}, H. J. Wang^{31,n,o}, H. P. Wang^{1,54}, K. Wang^{1,49}, L. L. Wang¹, M. Wang⁴¹, M. Z. Wang^{38,k}, Meng Wang^{1,54}, W. Wang⁵⁰, W. H. Wang⁶⁸, W. P. Wang^{63,49}, X. Wang^{38,k}, X. F. Wang^{31,n,o}, X. L. Wang^{9,h}, Y. Wang⁵⁰, Y. Wang^{63,49}, Y. D. Wang³⁷, Y. F. Wang^{1,49,54}, Y. Q. Wang¹, Y. Y. Wang^{31,n,o}, Z. Wang^{1,49}, Z. Y. Wang¹, Ziyi Wang⁵⁴,

Zongyuan Wang^{1,54}, D. H. Wei¹², F. Weidner⁶⁰, S. P. Wen¹, D. J. White⁵⁸, U. Wiedner⁴, G. Wilkinson⁶¹, M. Wolke⁶⁷, L. Wollenberg⁴, J. F. Wu^{1,54}, L. H. Wu¹, L. J. Wu^{1,54}, X. Wu^{9,h}, Z. Wu^{1,49}, L. Xia^{63,49}, H. Xiao^{9,h}, S. Y. Xiao¹, Z. J. Xiao³⁴, X. H. Xie^{38,k}, Y. G. Xie^{1,49}, Y. H. Xie⁶, T. Y. Xing^{1,54}, G. F. Xu¹, Q. J. Xu¹⁴, W. Xu^{1,54}, X. P. Xu⁴⁶, Y. C. Xu⁵⁴, F. Yan^{9,h}, L. Yan^{9,h}, W. B. Yan^{63,49}, W. C. Yan⁷¹, Xu Yan⁴⁶, H. J. Yang^{42,g}, H. X. Yang¹, L. Yang⁴³, S. L. Yang⁵⁴, Y. X. Yang¹², Yifan Yang^{1,54}, Zhi Yang²⁵, M. Ye^{1,49}, M. H. Ye⁷, J. H. Yin¹, Z. Y. You⁵⁰, B. X. Yu^{1,49,54}, C. X. Yu³⁶, G. Yu^{1,54}, J. S. Yu^{20,l}, T. Yu⁶⁴, C. Z. Yuan^{1,54}, L. Yuan², X. Q. Yuan^{38,k}, Y. Yuan¹, Z. Y. Yuan⁵⁰, C. X. Yue³², A. Yuncu^{53A,a}, A. A. Zafar⁶⁵, Zeng⁶, Y. Zeng^{20,l}, A. Q. Zhang¹, B. X. Zhang¹, Guangyi Zhang¹⁶, H. Zhang⁶³, H. H. Zhang²⁷, H. H. Zhang⁵⁰, H. Y. Zhang^{1,49}, J. J. Zhang⁴³, J. L. Zhang⁶⁹, J. Q. Zhang³⁴, J. W. Zhang^{1,49,54}, J. Y. Zhang¹, J. Z. Zhang^{1,54}, Jianyu Zhang^{1,54}, Jiawei Zhang^{1,54}, L. M. Zhang⁵², L. Q. Zhang⁵⁰, Lei Zhang³⁵, S. Zhang⁵⁰, S. F. Zhang³⁵, Shulei Zhang^{20,l}, X. D. Zhang³⁷, X. Y. Zhang⁴¹, Y. Zhang⁶¹, Y. H. Zhang^{1,49}, Y. T. Zhang^{63,49}, Yan Zhang^{63,49}, Yao Zhang¹, Yi Zhang^{9,h}, Z. H. Zhang⁶, Z. Y. Zhang⁶⁸, G. Zhao¹, J. Zhao³², J. Y. Zhao^{1,54}, J. Z. Zhao^{1,49}, Lei Zhao^{63,49}, Ling Zhao¹, M. G. Zhao³⁶, Q. Zhao¹, S. J. Zhao⁷¹, Y. B. Zhao^{1,49}, Y. X. Zhao²⁵, Z. G. Zhao^{63,49}, A. Zhemchugov^{29,b}, B. Zheng⁶⁴, J. P. Zheng^{1,49}, Y. Zheng^{38,k}, Y. H. Zheng⁵⁴, B. Zhong³⁴, C. Zhong⁶⁴, L. P. Zhou^{1,54}, Q. Zhou^{1,54}, X. Zhou⁶⁸, X. K. Zhou⁵⁴, X. R. Zhou^{63,49}, X. Y. Zhou³², A. N. Zhu^{1,54}, J. Zhu³⁶, K. Zhu¹, K. J. Zhu^{1,49,54}, S. H. Zhu⁶², T. J. Zhu⁶⁹, W. J. Zhu^{9,h}, W. J. Zhu³⁶, Y. C. Zhu^{63,49}, Z. A. Zhu^{1,54}, B. S. Zou¹, J. H. Zou¹

(BESIII Collaboration)

¹ Institute of High Energy Physics, Beijing 100049, People's Republic of China

² Beihang University, Beijing 100191, People's Republic of China

³ Beijing Institute of Petrochemical Technology, Beijing 102617, People's Republic of China

⁴ Bochum Ruhr-University, D-44780 Bochum, Germany

⁵ Carnegie Mellon University, Pittsburgh, Pennsylvania 15213, USA

⁶ Central China Normal University, Wuhan 430079, People's Republic of China

⁷ China Center of Advanced Science and Technology, Beijing 100190, People's Republic of China

⁸ COMSATS University Islamabad, Lahore Campus, Defence Road, Off Raiwind Road, 54000 Lahore, Pakistan

⁹ Fudan University, Shanghai 200443, People's Republic of China

¹⁰ G.I. Budker Institute of Nuclear Physics SB RAS (BINP), Novosibirsk 630090, Russia

¹¹ GSI Helmholtzcentre for Heavy Ion Research GmbH, D-64291 Darmstadt, Germany

¹² Guangxi Normal University, Guilin 541004, People's Republic of China

¹³ Guangxi University, Nanning 530004, People's Republic of China

¹⁴ Hangzhou Normal University, Hangzhou 310036, People's Republic of China

¹⁵ Helmholtz Institute Mainz, Staudinger Weg 18, D-55099 Mainz, Germany

¹⁶ Henan Normal University, Xinxiang 453007, People's Republic of China

¹⁷ Henan University of Science and Technology, Luoyang 471003, People's Republic of China

¹⁸ Huangshan College, Huangshan 245000, People's Republic of China

¹⁹ Hunan Normal University, Changsha 410081, People's Republic of China

²⁰ Hunan University, Changsha 410082, People's Republic of China

²¹ Indian Institute of Technology Madras, Chennai 600036, India

²² Indiana University, Bloomington, Indiana 47405, USA

²³ INFN Laboratori Nazionali di Frascati , (A)INFN Laboratori Nazionali di Frascati, I-00044, Frascati, Italy;

(B)INFN Sezione di Perugia, I-06100, Perugia, Italy; (C)University of Perugia, I-06100, Perugia, Italy

²⁴ INFN Sezione di Ferrara, (A)INFN Sezione di Ferrara, I-44122,

Ferrara, Italy; (B)University of Ferrara, I-44122, Ferrara, Italy

²⁵ Institute of Modern Physics, Lanzhou 730000, People's Republic of China

²⁶ Institute of Physics and Technology, Peace Ave. 54B, Ulaanbaatar 13330, Mongolia

²⁷ Jilin University, Changchun 130012, People's Republic of China

²⁸ Johannes Gutenberg University of Mainz, Johann-Joachim-Becher-Weg 45, D-55099 Mainz, Germany

²⁹ Joint Institute for Nuclear Research, 141980 Dubna, Moscow region, Russia

³⁰ Justus-Liebig-Universitaet Giessen, II. Physikalisches Institut, Heinrich-Buff-Ring 16, D-35392 Giessen, Germany

³¹ Lanzhou University, Lanzhou 730000, People's Republic of China

³² Liaoning Normal University, Dalian 116029, People's Republic of China

- ³³ Liaoning University, Shenyang 110036, People's Republic of China
³⁴ Nanjing Normal University, Nanjing 210023, People's Republic of China
³⁵ Nanjing University, Nanjing 210093, People's Republic of China
³⁶ Nankai University, Tianjin 300071, People's Republic of China
³⁷ North China Electric Power University, Beijing 102206, People's Republic of China
³⁸ Peking University, Beijing 100871, People's Republic of China
³⁹ Qufu Normal University, Qufu 273165, People's Republic of China
⁴⁰ Shandong Normal University, Jinan 250014, People's Republic of China
⁴¹ Shandong University, Jinan 250100, People's Republic of China
⁴² Shanghai Jiao Tong University, Shanghai 200240, People's Republic of China
⁴³ Shanxi Normal University, Linfen 041004, People's Republic of China
⁴⁴ Shanxi University, Taiyuan 030006, People's Republic of China
⁴⁵ Sichuan University, Chengdu 610064, People's Republic of China
⁴⁶ Soochow University, Suzhou 215006, People's Republic of China
⁴⁷ South China Normal University, Guangzhou 510006, People's Republic of China
⁴⁸ Southeast University, Nanjing 211100, People's Republic of China
⁴⁹ State Key Laboratory of Particle Detection and Electronics,
Beijing 100049, Hefei 230026, People's Republic of China
⁵⁰ Sun Yat-Sen University, Guangzhou 510275, People's Republic of China
⁵¹ Suranaree University of Technology, University Avenue 111, Nakhon Ratchasima 30000, Thailand
⁵² Tsinghua University, Beijing 100084, People's Republic of China
⁵³ Turkish Accelerator Center Particle Factory Group, (A)Istanbul Bilgi University, 34060
Eyup, Istanbul, Turkey; (B)Near East University, Nicosia, North Cyprus, Mersin 10, Turkey
⁵⁴ University of Chinese Academy of Sciences, Beijing 100049, People's Republic of China
⁵⁵ University of Groningen, NL-9747 AA Groningen, The Netherlands
⁵⁶ University of Hawaii, Honolulu, Hawaii 96822, USA
⁵⁷ University of Jinan, Jinan 250022, People's Republic of China
⁵⁸ University of Manchester, Oxford Road, Manchester, M13 9PL, United Kingdom
⁵⁹ University of Minnesota, Minneapolis, Minnesota 55455, USA
⁶⁰ University of Muenster, Wilhelm-Klemm-Str. 9, 48149 Muenster, Germany
⁶¹ University of Oxford, Keble Rd, Oxford, UK OX13RH
⁶² University of Science and Technology Liaoning, Anshan 114051, People's Republic of China
⁶³ University of Science and Technology of China, Hefei 230026, People's Republic of China
⁶⁴ University of South China, Hengyang 421001, People's Republic of China
⁶⁵ University of the Punjab, Lahore-54590, Pakistan
⁶⁶ University of Turin and INFN, (A)University of Turin, I-10125, Turin, Italy; (B)University
of Eastern Piedmont, I-15121, Alessandria, Italy; (C)INFN, I-10125, Turin, Italy
⁶⁷ Uppsala University, Box 516, SE-75120 Uppsala, Sweden
⁶⁸ Wuhan University, Wuhan 430072, People's Republic of China
⁶⁹ Xinyang Normal University, Xinyang 464000, People's Republic of China
⁷⁰ Zhejiang University, Hangzhou 310027, People's Republic of China
⁷¹ Zhengzhou University, Zhengzhou 450001, People's Republic of China
^a Also at Bogazici University, 34342 Istanbul, Turkey
^b Also at the Moscow Institute of Physics and Technology, Moscow 141700, Russia
^c Also at the Novosibirsk State University, Novosibirsk, 630090, Russia
^d Also at the NRC "Kurchatov Institute", PNPI, 188300, Gatchina, Russia
^e Also at Istanbul Arel University, 34295 Istanbul, Turkey
^f Also at Goethe University Frankfurt, 60323 Frankfurt am Main, Germany
^g Also at Key Laboratory for Particle Physics, Astrophysics and Cosmology, Ministry
of Education; Shanghai Key Laboratory for Particle Physics and Cosmology; Institute
of Nuclear and Particle Physics, Shanghai 200240, People's Republic of China

^h Also at Key Laboratory of Nuclear Physics and Ion-beam Application (MOE) and Institute of Modern Physics, Fudan University, Shanghai 200443, People's Republic of China

ⁱ Also at Harvard University, Department of Physics, Cambridge, MA, 02138, USA

^j Currently at: Institute of Physics and Technology, Peace Ave.54B, Ulaanbaatar 13330, Mongolia

^k Also at State Key Laboratory of Nuclear Physics and Technology,

Peking University, Beijing 100871, People's Republic of China

^l School of Physics and Electronics, Hunan University, Changsha 410082, China

^m Also at Guangdong Provincial Key Laboratory of Nuclear Science, Institute of Quantum Matter, South China Normal University, Guangzhou 510006, China

ⁿ Frontier Science Center for Rare Isotopes, Lanzhou University, Lanzhou 730000, People's Republic of China

^o Lanzhou Center for Theoretical Physics, Lanzhou University, Lanzhou 730000, People's Republic of China

By analyzing an e^+e^- annihilation data sample corresponding to an integrated luminosity of 2.93 fb^{-1} collected at a center-of-mass energy of 3.773 GeV with the BESIII detector, we measure the branching fraction of the $D^0 \rightarrow \rho^-\mu^+\nu_\mu$ decay for the first time. We obtain $\mathcal{B}_{D^0 \rightarrow \rho^-\mu^+\nu_\mu} = (1.35 \pm 0.09_{\text{stat}} \pm 0.09_{\text{syst}}) \times 10^{-3}$. Combining with theoretical predictions, we extract the CKM matrix element $|V_{cd}| = 0.204 \pm 0.007_{\text{stat}} \pm 0.007_{\text{syst}} \pm 0.014_{\text{theory}}$. Using the world average of $\mathcal{B}_{D^0 \rightarrow \rho^-e^+\nu_e}$, we find a branching fraction ratio of $\mathcal{B}_{D^0 \rightarrow \rho^-\mu^+\nu_\mu}/\mathcal{B}_{D^0 \rightarrow \rho^-e^+\nu_e} = 0.90 \pm 0.11$, which agrees with the theoretical expectation of lepton flavor universality within the uncertainty. Combining the world average of $\mathcal{B}_{D^+ \rightarrow \rho^0\mu^+\nu_\mu}$ and the lifetimes of $D^{0(+)}$, we obtain a partial decay width ratio of $\Gamma_{D^0 \rightarrow \rho^-\mu^+\nu_\mu}/(2\Gamma_{D^+ \rightarrow \rho^0\mu^+\nu_\mu}) = 0.71 \pm 0.14$, which is consistent with the isospin symmetry expectation of one within 2.1σ . For the reported values of $\mathcal{B}_{D^0 \rightarrow \rho^-\mu^+\nu_\mu}/\mathcal{B}_{D^0 \rightarrow \rho^-e^+\nu_e}$ and $\Gamma_{D^0 \rightarrow \rho^-\mu^+\nu_\mu}/2\Gamma_{D^+ \rightarrow \rho^0\mu^+\nu_\mu}$, the uncertainty is the quadratic sum of the statistical and systematic uncertainties.

PACS numbers: 13.20.Fc, 12.15.Hh

Lepton flavor universality (LFU) is usually thought of as a basic property of the Standard Model (SM) [1–4]. It postulates that the couplings between the three families of leptons and gauge bosons do not depend on the lepton flavor. Experimental studies of semileptonic decays of pseudoscalar mesons are important to test LFU and explore possible new physics. Since 2012, tests of LFU have been carried out in several semileptonic B decays at BaBar, Belle, and LHCb. The measured branching fraction ratios $\mathcal{R}_{\tau/\ell}^{\bar{D}^{(*)}} = \mathcal{B}_{B \rightarrow \bar{D}^{(*)}\tau^+\nu_\tau}/\mathcal{B}_{B \rightarrow \bar{D}^{(*)}\ell^+\nu_\ell}$ ($\ell = \mu, e$) [5–11] indicate a 3.1σ deviation from the value predicted in the SM [12]. This tension stimulated development of various theoretical models [2, 13–17]. In this context, investigations of exclusive semileptonic D decays give important complementary tests of LFU. In recent years, BESIII reported tests of μ - e LFU with the semileptonic decays $D \rightarrow X\ell^+\nu_\ell$ ($X = \bar{K}, \pi, \omega$, and η) [18–22]. For each decay, the difference between the measured branching fraction ratio ($\mathcal{R}_{\mu/e}^X = \mathcal{B}_{D \rightarrow X\mu^+\nu_\mu}/\mathcal{B}_{D \rightarrow Xe^+\nu_e}$) and the corresponding SM prediction is less than 1.7σ . The decay $D^0 \rightarrow \rho^-\mu^+\nu_\mu$, calculated using the quark potential model in 1989 [23], has not yet been measured. Observation of this decay and verification of the SM prediction for $\mathcal{R}_{\mu/e}^{\rho^-}$ offer a crucial LFU test.

In addition to the quark potential model work [23], the branching fraction of $D^0 \rightarrow \rho^-\mu^+\nu_\mu$ has been calculated using QCD light-cone sum rules (LCSR) [24,

25], the light-front quark model (LFQM) [26], the covariant confined quark model (CCQM) [27, 28], the chiral unitarity approach (χ UA) [29], and the relativistic quark model (RQM) [30]. The predicted branching fractions range from $(1.55 - 2.01) \times 10^{-3}$. This decay also provides an opportunity to determine the $c \rightarrow d$ Cabibbo-Kobayashi-Maskawa (CKM) matrix element $|V_{cd}|$. Furthermore, the measured branching fraction helps constrain lattice QCD calculations on the hadronic form factors of semileptonic D and B decays. More precise calculations of branching fractions and hadronic form factors are key inputs in the determination of CKM parameters [31–34] which allow important tests of CKM matrix unitarity.

Under the assumption of isospin symmetry, the partial width ratio $\mathcal{R}_{\text{IS}}^{\rho,\ell} = \Gamma_{D^0 \rightarrow \rho^-\ell^+\nu_\mu}/2\Gamma_{D^+ \rightarrow \rho^0\ell^+\nu_\mu} = (\mathcal{B}_{D^0 \rightarrow \rho^-\ell^+\nu_\mu} \cdot \tau_{D^0})/(2\mathcal{B}_{D^+ \rightarrow \rho^0\ell^+\nu_\mu} \cdot \tau_{D^0})$ is expected to be unity. Here, $\tau_{D^{0(+)}}$ is the lifetime of the $D^{0(+)}$ meson. Using the world average values [35], one obtains $\mathcal{R}_{\text{IS}}^{\rho,e} = 0.87 \pm 0.13$, which agrees with unity within the uncertainty. A measurement of the branching fraction of the decay $D^0 \rightarrow \rho^-\mu^+\nu_\mu$ allows a determination of $\mathcal{R}_{\text{IS}}^{\rho,\mu}$ which tests isospin symmetry in $D^{0(+)} \rightarrow \rho^{-(0)}\ell^+\nu_\ell$ decays.

Using a data sample corresponding to an integrated luminosity of 2.93 fb^{-1} [36] taken at a center-of-mass energy of 3.773 GeV with the BESIII detector, we report the first observation and a branching fraction measurement of $D^0 \rightarrow \rho^-\mu^+\nu_\mu$, a determination of

$|V_{cd}|$ and tests of both LFU with $D^0 \rightarrow \rho^- \ell^+ \nu_\ell$ decays and isospin symmetry in $D^{0(+)} \rightarrow \rho^{-(0)} \mu^+ \nu_\mu$ decays. Throughout this Letter, charge conjugate channels are always implied and ρ denotes the $\rho(770)$.

Details about the design and performance of the BESIII detector are given in Ref. [37]. Monte Carlo (MC) simulated data samples, produced with a GEANT4-based [38] software package including the geometric description of the BESIII detector and the detector response, are used to determine the detection efficiency and to estimate the backgrounds. The simulation includes the beam-energy spread and initial-state radiation in the e^+e^- annihilations modeled with the generator KKMC [39]. The inclusive MC sample consists of the production of $D\bar{D}$ pairs with consideration of quantum coherence for all neutral D modes, the non- $D\bar{D}$ decays of the $\psi(3770)$, the initial-state radiation production of the J/ψ and $\psi(3686)$ states, and the continuum processes. The known decay modes are modeled with EVTGEN [40] using the branching fractions taken from the Particle Data Group [35], and the remaining unknown decays from the charmonium states are modeled with LUNDCHARM [41]. Final state radiation from charged final state particles is incorporated with the PHOTOS package [42]. The vector hadronic form factors of the semileptonic decay $D^0 \rightarrow \rho^- \mu^+ \nu_\mu$ are simulated with those of the $D^0 \rightarrow \rho^- e^+ \nu_e$ decay [43].

At the center-of-mass energy of 3.773 GeV, D^0 and \bar{D}^0 mesons are produced in pairs without additional hadrons. This feature results in an ideal environment to study D^0 decays with the double-tag (DT) method. At first, the single-tag (ST) \bar{D}^0 meson is reconstructed using the hadronic decays $\bar{D}^0 \rightarrow K^+ \pi^-$, $K^+ \pi^- \pi^0$, and $K^+ \pi^- \pi^- \pi^+$. Then, the DT candidate events, in which a $D^0 \rightarrow \rho^- \mu^+ \nu_\mu$ decay candidate is found in the system recoiling against an ST \bar{D}^0 meson, are selected. The branching fraction of the $D^0 \rightarrow \rho^- \mu^+ \nu_\mu$ decay is determined by

$$\mathcal{B}_{D^0 \rightarrow \rho^- \mu^+ \nu_\mu} = N_{\text{DT}} / (N_{\text{ST}}^{\text{tot}} \cdot \varepsilon_{D^0 \rightarrow \rho^- \mu^+ \nu_\mu}), \quad (1)$$

where $N_{\text{ST}}^{\text{tot}}$ and N_{DT} are the yields of the ST and DT candidates in data, respectively. Here, $\varepsilon_{D^0 \rightarrow \rho^- \mu^+ \nu_\mu} = \sum_i [(\varepsilon_{\text{DT}}^i \cdot N_{\text{ST}}^i) / (\varepsilon_{\text{ST}}^i \cdot N_{\text{ST}}^{\text{tot}})]$ is the effective signal efficiency of finding $D^0 \rightarrow \rho^- \mu^+ \nu_\mu$ in the presence of the ST \bar{D}^0 meson, where ε_{ST} and ε_{DT} are the detection efficiencies of the ST and DT candidates, respectively, and i labels the ST modes.

In this analysis, the selection criteria for K^\pm , π^\pm , γ , and π^0 candidates follow those employed in Refs. [19–22, 44, 46–51]. All charged tracks are required to be within the polar angle range $|\cos \theta| < 0.93$, and their distance of closest approach to the interaction point perpendicular to and along the MDC axis are required to be smaller than 1 cm and 10 cm, respectively. Charged kaons and pions are identified using the combined information from

the specific energy loss (dE/dx) in the drift chamber and information from the time-of-flight system (TOF), via combined confidence levels for the pion and kaon hypotheses. Those charged tracks with larger confidence level for the kaon (pion) hypothesis are identified as kaon (pion) candidates.

Candidates for neutral pions are reconstructed from pairs of photons that satisfy the following selection criteria. Photon candidates are chosen from isolated clusters in the electromagnetic calorimeter (EMC) whose energies are larger than 25 (50) MeV if the crystal with the maximum deposited energy in that cluster is in the barrel (endcap) region [37]. To reject photons from bremsstrahlung and from interactions with material, showers within a cone angle of 10° around the extrapolated position on the EMC of any charged track are rejected. The energy deposited in the TOF counters is taken into account to improve the reconstruction efficiency and energy resolution. Reconstructed showers due to electronic noise or beam backgrounds are suppressed by limiting the cluster time to be within (0, 700) ns after the event start time. Photon pairs with invariant mass in the range $(0.115, 0.150) \text{ GeV}/c^2$ are retained as π^0 candidates. To improve the momentum resolution, a one-constraint kinematic fit to the nominal π^0 mass [35] is imposed on these photon pairs.

For the $\bar{D}^0 \rightarrow K^+ \pi^-$ tag mode, backgrounds related to cosmic rays and Bhabha scattering events are vetoed by using the requirements described in Ref. [52]. To distinguish the ST \bar{D}^0 mesons from combinatorial backgrounds, we define the energy difference $\Delta E \equiv E_{\bar{D}^0} - E_{\text{beam}}$ and the beam-constrained mass $M_{\text{BC}} \equiv \sqrt{E_{\text{beam}}^2/c^4 - |\vec{p}_{\bar{D}^0}|^2/c^2}$, where E_{beam} is the beam energy, and $E_{\bar{D}^0}$ and $\vec{p}_{\bar{D}^0}$ are the total energy and momentum of the ST \bar{D}^0 candidate in the e^+e^- center-of-mass frame, respectively. When multiple combinations for an ST mode are present in an event, the combination with the smallest $|\Delta E|$ per tag mode per charge is retained for further analysis. The ST candidates are required to be within $\Delta E \in (-0.055, +0.040) \text{ GeV}$ for $\bar{D}^0 \rightarrow K^+ \pi^- \pi^0$ and $\Delta E \in (-0.025, +0.025) \text{ GeV}$ for $\bar{D}^0 \rightarrow K^+ \pi^-$ and $\bar{D}^0 \rightarrow K^+ \pi^- \pi^- \pi^+$.

Figure 1 shows the M_{BC} distributions of the accepted ST \bar{D}^0 candidates. For each tag mode, the yield of ST \bar{D}^0 mesons is obtained from a maximum likelihood fit to the M_{BC} distribution of the accepted candidates. In the fit, the signal and background are described by the signal shape from MC simulation and an ARGUS function [53], respectively. To compensate for offsets in calibration and resolution differences between data and MC simulation, the signal shape is convolved with a double-Gaussian function. The means, widths and relative fractions of the Gaussian components are free parameters in the fit. The resulting fits to the M_{BC} distributions are also shown in Fig. 1. Candidates in the M_{BC} mass window $(1.859, 1.873) \text{ GeV}/c^2$ are kept

for further analysis. For each tag mode, the yield of the ST \bar{D}^0 mesons is obtained by integrating the fitted signal shape over the M_{BC} mass window. The total yield of ST \bar{D}^0 mesons is $N_{\text{ST}}^{\text{tot}} = (232.1 \pm 0.2_{\text{stat}}) \times 10^4$.

In the presence of the ST \bar{D}^0 mesons, candidates for $D^0 \rightarrow \rho^- \mu^+ \nu_\mu$ are selected from the tracks and showers which have not been used in the tag reconstruction. The ρ^- candidates are reconstructed via the $\rho^- \rightarrow \pi^- \pi^0$ decay. The selection criteria of π^- and π^0 candidates are the same as those used in the ST selection. The invariant mass of the $\pi^- \pi^0$ candidate is required to be within $(0.625, 0.925) \text{ GeV}/c^2$. To suppress the background from hadronic $D^{0(+)}$ decays, it is required that there is no additional charged track or π^0 except for those used to form the signal and ST candidates.

The combined dE/dx , TOF, and EMC information is used to identify the muon candidates. The combined confidence levels for various particle hypotheses are calculated. Charged tracks are identified as muons if the confidence level for the muon hypothesis is larger than 0.001 and also larger than those of the electron and kaon hypotheses. To reduce misidentification of hadrons as muons, the deposited energy in the EMC of the muon candidate ($E_{\mu, \text{EMC}}$) is required to be in the range $(0.125, 0.275) \text{ GeV}$.

The signal yield of the $D^0 \rightarrow \rho^- \mu^+ \nu_\mu$ decay is determined by a kinematic quantity defined as $M_{\text{miss}}^2 \equiv E_{\text{miss}}^2/c^4 - |\vec{p}_{\text{miss}}|^2/c^2$, which is expected to peak around zero for correctly reconstructed signal events. Here, $E_{\text{miss}} \equiv E_{\text{beam}} - E_{\rho^-} - E_{\mu^+}$ and $\vec{p}_{\text{miss}} \equiv \vec{p}_{D^0} - \vec{p}_{\rho^-} - \vec{p}_{\mu^+}$ are the missing energy and momentum of the DT event in the $e^+ e^-$ center-of-mass frame, in which $E_{\rho^- (\mu^+)}$ and $\vec{p}_{\rho^- (\mu^+)}$ are the energy and momentum of the $\rho^- (\mu^+)$ candidates. The M_{miss}^2 resolution is improved using $\vec{p}_{D^0} \equiv -\hat{\vec{p}}_{\bar{D}^0} \cdot \sqrt{E_{\text{beam}}^2/c^2 - m_{D^0}^2 c^2}$, where $\hat{\vec{p}}_{\bar{D}^0}$ is the unit vector in the momentum direction of the ST \bar{D}^0 and m_{D^0} is the D^0 nominal mass [35].

The selected sample is contaminated by background events with correctly reconstructed ST mesons but mis-reconstructed signal decays which can peak in the M_{miss}^2 distribution. In order to reject such peaking background from the hadronic decays $D^0 \rightarrow K_S^0(\pi^0 \pi^0) \pi^+ \pi^-$ and $D^0 \rightarrow K_S^0(\pi^+ \pi^-) \pi^0 (\pi^0)$, the mass recoiling against the $D^0 \pi_{\mu \rightarrow \pi}^+ \pi^-$ system and the invariant mass of the $\pi_{\mu \rightarrow \pi}^+ \pi^-$ combination are required to be outside $(0.458, 0.538) \text{ GeV}/c^2$ and $(0.468, 0.528) \text{ GeV}/c^2$, respectively, where $\pi_{\mu \rightarrow \pi}^+$ denotes a track identified as a muon candidate whose mass has been replaced by the π^+ mass. To reduce the peaking background from $D^0 \rightarrow \pi^+ \pi^- \pi^0$, the invariant mass of the $\rho^- \mu^+$ combination ($M_{\rho^- \mu^+}$) is required to be less than $1.5 \text{ GeV}/c^2$. To suppress the peaking background from $D^0 \rightarrow \pi^+ \pi^- \pi^0$, the maximum energy of any photon that is not used in the DT selection ($E_{\text{extra } \gamma}^{\text{max}}$) is required to be less than 0.25 GeV . The remaining

peaking background events are mainly from D^0 decays into $\pi^+ \pi^- \pi^0 \pi^0$ final states, including $D^0 \rightarrow K_S^0(\pi^0 \pi^0) \pi^+ \pi^-$, $D^0 \rightarrow K_S^0(\pi^+ \pi^-) \pi^0 \pi^0$, $D^0 \rightarrow K^-(\pi^- \pi^0) \pi^+ \pi^0$, and $D^0 \rightarrow \pi^+ \pi^- \pi^0 \pi^0|_{\text{non-}K}$. Since there is little difference in their M_{miss}^2 shape, these four components are combined together, and will be called $D^0 \rightarrow \pi^+ \pi^- \pi^0 \pi^0$. The remaining background events from $D^0 \rightarrow K_S^0(\pi^+ \pi^-) \pi^0$, and $D^0 \rightarrow \pi^+ \pi^- \pi^0$ are negligible and have been combined into the combinatorial background in further analysis.

To suppress the background from $D^0 \rightarrow \bar{K}^*(892)^-(K^- \pi^0) \mu^+ \nu_\mu$, the candidate events are further required not to be within the range $|M_{\text{miss } \pi^- \rightarrow K^-}^2| < 0.05 \text{ GeV}^2/c^4$, where $M_{\text{miss } \pi^- \rightarrow K^-}^2$ is the M_{miss}^2 value calculated by replacing the mass of the charged pion candidate with the kaon mass in the calculation of M_{miss}^2 .

Figure 2 shows the M_{miss}^2 distribution of the accepted DT events in data. The semileptonic decay yield is obtained from an unbinned maximum likelihood fit to the M_{miss}^2 distribution. In the fit, the semileptonic signal is modeled by the MC-simulated shape convolved with a Gaussian function describing differences in resolution and calibration between data and MC simulation. The parameters of this Gaussian function are fixed to the values obtained from a similar fit to $D^0 \rightarrow \rho^- e^+ \nu_e$ candidate events. The peaking background of $D^0 \rightarrow \pi^+ \pi^- \pi^0 \pi^0$ is modeled by the M_{miss}^2 shape derived from the $D^0 \rightarrow \pi^+ \pi^- \pi^0 \pi^0$ control sample in data, in which one π^0 is removed and the π^+ mass is replaced by the μ^+ mass. The non-peaking backgrounds, including the contribution from wrongly reconstructed ST candidates, are described by the MC-simulated shape obtained from the inclusive MC sample. The yields of the signal, peaking background, and non-peaking backgrounds are free parameters in the fit. The fit result is also shown in Fig. 2. From the fit, we obtain the signal yield of $D^0 \rightarrow \rho^- \mu^+ \nu_\mu$ to be $N_{\text{DT}} = 570 \pm 40_{\text{stat}}$ and the yield of the peaking background of $D^0 \rightarrow \pi^+ \pi^- \pi^0 \pi^0$ to be 373 ± 36 . The statistical significance, calculated by $\sqrt{-2\ln(\mathcal{L}_0/\mathcal{L}_{\text{max}})}$, is greater than 10σ . Here, \mathcal{L}_{max} and \mathcal{L}_0 are the maximum likelihoods of the fits with and without the signal component, respectively, and the difference in the number of fit parameters is one.

The tag-related values N_{ST}^i , ϵ_{ST}^i , and ϵ_{DT}^i are summarized in Table 1. The average efficiency of detecting $D^0 \rightarrow \rho^- \mu^+ \nu_\mu$ decays is $\varepsilon_{D^0 \rightarrow \rho^- \mu^+ \nu_\mu} = (18.22 \pm 0.13_{\text{stat}})\%$ which includes the branching fraction of $\pi^0 \rightarrow \gamma\gamma$. The kinematic distributions of the $D^0 \rightarrow \rho^- \mu^+ \nu_\mu$ candidate events agree well between data and MC simulation.

Inserting N_{DT} , $\varepsilon_{D^0 \rightarrow \rho^- \mu^+ \nu_\mu}$, and $N_{\text{ST}}^{\text{tot}}$ into Eq. (1), we obtain

$$\mathcal{B}_{D^0 \rightarrow \rho^- \mu^+ \nu_\mu} = (1.35 \pm 0.09 \pm 0.09) \times 10^{-4},$$

where the first uncertainty is statistical and the second

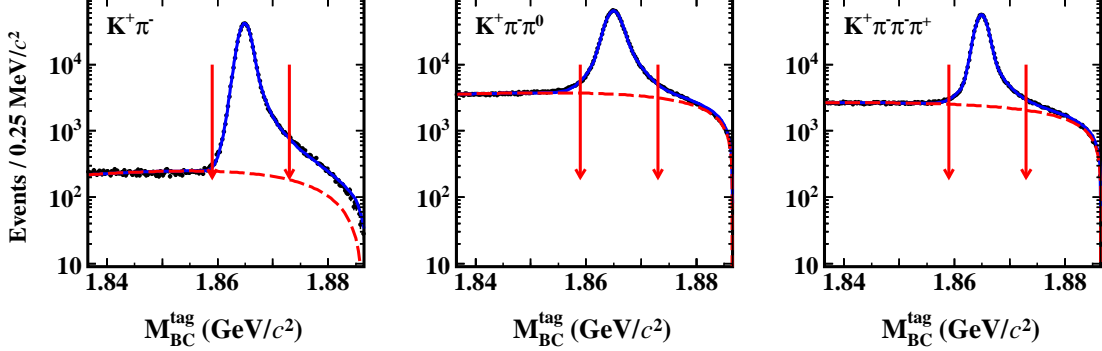


Fig. 1. Fits to the M_{BC} distributions of the ST \bar{D}^0 candidates. Data are shown as dots (uncertainties are not visible at this scale). The solid blue and dashed red curves are the fit results and the fitted backgrounds, respectively. Pairs of red arrows indicate the M_{BC} selection.

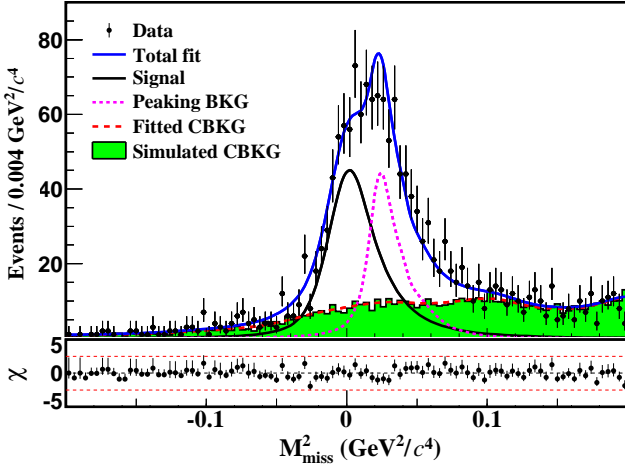


Fig. 2. Fit to the M_{miss}^2 distribution of the accepted candidate events for $D^+ \rightarrow \rho^-\mu^+\nu_\mu$ in data (points with error bars). The solid blue curve is the fit result, the solid black curve is the semileptonic signal, the dashed pink curve is the peaking background (Peaking BKG) of $D^0 \rightarrow \pi^+\pi^-\pi^0\pi^0$, and the dashed red curve is the fitted combinatorial background (Fitted CBKG). The filled green histogram is the simulated combinatorial background (Simulated CBKG) from inclusive MC sample.

Table 1. The ST \bar{D}^0 yields in data (N_{ST}^i), the ST efficiencies (ϵ_{ST}^i) and the DT efficiencies (ϵ_{DT}^i). The uncertainties are statistical only.

D^0 mode i	N_{ST}^i	ϵ_{ST}^i (%)	ϵ_{DT}^i (%)
$K^+\pi^-$	$516\,971 \pm 746$	64.28 ± 0.09	12.87 ± 0.11
$K^+\pi^-\pi^0$	$1\,099\,361 \pm 1327$	36.35 ± 0.04	6.95 ± 0.08
$K^+\pi^-\pi^-\pi^+$	$704\,677 \pm 1094$	40.26 ± 0.07	6.25 ± 0.08

is systematic as discussed below.

In the branching fraction measurement with the DT method, most uncertainties related to the ST selection cancel. Systematic uncertainties arise from the following

sources. The uncertainty in the total yield of ST \bar{D}^0 mesons has been studied in Refs. [19, 20, 44] and is 0.5%. The systematic uncertainties originating from the tracking and PID efficiencies of π^\pm are 0.3% and 0.2% per pion, respectively, based on an analysis of DT $D\bar{D}$ hadronic events [45]. The muon tracking and PID efficiencies are studied by analyzing $e^+e^- \rightarrow \gamma\mu^+\mu^-$ events. Here, the muon identification efficiencies include the $E_{\mu,\text{EMC}}$ requirement. Using this control sample, data-MC differences are studied in the two-dimensional momentum versus $\cos\theta$ plane. We re-weight using these data-MC differences, accounting for the different distribution of events in these two variables for the $D^0 \rightarrow \rho^-\mu^+\nu_\mu$ signal decays. Systematic uncertainties are obtained as the integral over the re-weighted two-dimensional distribution, giving 0.2% and 0.2% per muon for the muon tracking and PID efficiencies, respectively. The uncertainty of the π^0 reconstruction is studied with DT $D\bar{D}$ hadronic decays of $D^0 \rightarrow K^-\pi^+$, $K^-\pi^+\pi^+\pi^-$ versus $\bar{D}^0 \rightarrow K^+\pi^-\pi^0$, $K_S^0\pi^0$ [19, 44] and is found to be 0.6%. The uncertainty of the combined $E_{\text{extra}}^{\max}\gamma$ and $N_{\text{extra}}\pi^0$ requirements is estimated to be 1.3% by analyzing the DT candidate events of $D^0 \rightarrow \pi^-\pi^0e^+\nu_e$. The uncertainty of the M_{miss}^2 fit is found to be 6.6% by examining the branching fraction changes with an alternative signal shape without Gaussian smearing of the MC-simulated signal shape (0.9%), an MC-simulated shape of the peaking background of $D^0 \rightarrow \pi^+\pi^-\pi^0\pi^0$ (5.3%), and combinatorial background shapes after varying the quoted branching fractions by $\pm 1\sigma$ for the two main combinatorial components of $D^0 \rightarrow K_S^0\pi^+\pi^-\pi^0$ and $D^0 \rightarrow K^*(892)^-\mu^+\nu_\mu$ (3.8%). The uncertainty arising from the finite MC statistics used to determine the efficiencies is 0.7%. The uncertainty due to the signal MC model is 0.3%, determined by the difference between our nominal DT efficiency and that determined by varying the input form factors by $\pm 1\sigma$. Systematic uncertainties from other selection criteria are

found to be negligible. Adding these uncertainties in quadrature yields a total systematic uncertainty of 6.8%. The systematic uncertainties are summarized in Table 2.

Table 2. Relative systematic uncertainties in the branching fraction measurement.

Source	Uncertainty (%)
$N_{\text{ST}}^{\text{tot}}$	0.5
π^- tracking	0.3
π^- PID	0.2
μ^+ tracking	0.2
μ^+ PID	0.2
π^0 reconstruction	0.6
$E_{\text{extra } \gamma}^{\text{max}}$ and $N_{\text{extra } \pi^0}$ requirements	1.3
M_{miss}^2 fit	6.6
MC statistics	0.7
MC model	0.3
Total	6.8

In summary, the semileptonic decay $D^0 \rightarrow \rho^- \mu^+ \nu_\mu$ has been observed for the first time. The absolute branching fraction of this decay is determined to be $\mathcal{B}_{D^0 \rightarrow \rho^- \mu^+ \nu_\mu} = (1.35 \pm 0.09_{\text{stat}} \pm 0.09_{\text{syst}}) \times 10^{-3}$. Table 3 shows comparisons of the measured and predicted branching fractions for $D^0 \rightarrow \rho^- \mu^+ \nu_\mu$. Using the world average value of $\mathcal{B}_{D^0 \rightarrow \rho^- e^+ \nu_e} = (1.50 \pm 0.12) \times 10^{-3}$ [35], we obtain the branching fraction ratio $R_{\mu/e} = \mathcal{B}_{D^0 \rightarrow \rho^- \mu^+ \nu_e} / \mathcal{B}_{D^0 \rightarrow \rho^- e^+ \nu_e} = 0.90 \pm 0.11$. This result agrees with the SM predictions 0.93–0.96 [24, 26–30]. Our result is consistent with LFU in $D^0 \rightarrow \rho^- \ell^+ \nu_\ell$ decays. Using the branching fraction predicted in Ref. [25], which is closest to the measured value, we obtain $|V_{cd}| = 0.204 \pm 0.007_{\text{stat}} \pm 0.007_{\text{syst}} \pm 0.014_{\text{theory}}$. The obtained value of $|V_{cd}|$ is consistent with the results measured with other processes [22, 54–57] and is a valuable complementary input to test the unitarity of the CKM matrix. Combining the world averages of $\mathcal{B}_{D^+ \rightarrow \rho^0 \mu^+ \nu_\mu}$, τ_{D^0} , and τ_{D^+} [35], we determine $\mathcal{R}_{\text{IS}}^{\rho, \mu} = 0.71 \pm 0.14$. This ratio deviates from unity based on isospin symmetry at the level of 2.1σ . Improved measurements of $D^0 \rightarrow \rho^- \mu^+ \nu_\mu$ and $D^+ \rightarrow \rho^0 \mu^+ \nu_\mu$ with larger data samples [58, 59] in the near future will be crucial to clarify this tension.

The BESIII collaboration thanks the staff of BEPCII and the IHEP computing center for their strong support. This work is supported in part by National Key Research and Development Program of China under Contracts Nos. 2020YFA0406400, 2020YFA0406300; National Natural Science Foundation of China (NSFC) under Contracts Nos. 11775230, 11625523, 11635010, 11735014, 11822506, 11835012, 11935015, 11935016, 11935018, 11961141012; the Chinese Academy of Sciences (CAS) Large-Scale Scientific Facility Program; Joint Large-Scale Scientific Facility Funds of the NSFC and CAS under Contracts Nos. U1932102, U1732263, U1832207;

CAS Key Research Program of Frontier Sciences under Contracts Nos. QYZDJ-SSW-SLH003, QYZDJ-SSW-SLH040; 100 Talents Program of CAS; INPAC and Shanghai Key Laboratory for Particle Physics and Cosmology; ERC under Contract No. 758462; European Union Horizon 2020 research and innovation programme under Contract No. Marie Skłodowska-Curie grant agreement No 894790; German Research Foundation DFG under Contracts Nos. 443159800, Collaborative Research Center CRC 1044, FOR 2359, GRK 214; Istituto Nazionale di Fisica Nucleare, Italy; Ministry of Development of Turkey under Contract No. DPT2006K-120470; National Science and Technology fund; Olle Engkvist Foundation under Contract No. 200-0605; STFC (United Kingdom); The Knut and Alice Wallenberg Foundation (Sweden) under Contract No. 2016.0157; The Royal Society, UK under Contracts Nos. DH140054, DH160214; The Swedish Research Council; U. S. Department of Energy under Contracts Nos. DE-FG02-05ER41374, DE-SC-0012069.

-
- [1] A. Salam and J. C. Ward, *Phys. Lett.* **13**, 168 (1964).
 - [2] S. Fajfer, J. F. Kamenik, I. Nisandzic, and U. Rojec, *Phys. Rev. Lett.* **109**, 161801 (2012).
 - [3] S. Fajfer, I. Nisandzic, and U. Rojec, *Phys. Rev. D* **91**, 094009 (2015).
 - [4] X. D. Guo, X. Q. Hao, H. W. Ke, M. G. Zhao, and X. Q. Li, *Chin. Phys. C* **41**, 093107 (2017).
 - [5] J. P. Lees *et al.* (BaBar Collaboration), *Phys. Rev. Lett.* **109**, 101802 (2012).
 - [6] J. P. Lees *et al.* (BaBar Collaboration), *Phys. Rev. D* **88**, 072012 (2013).
 - [7] R. Aaij *et al.* (LHCb Collaboration), *Phys. Rev. Lett.* **115**, 111803 (2015).
 - [8] M. Huschle *et al.* (Belle Collaboration), *Phys. Rev. D* **92**, 072014 (2015).
 - [9] Y. Sato *et al.* (Belle Collaboration), *Phys. Rev. D* **94**, 072007 (2016).
 - [10] R. Aaij *et al.* (LHCb Collaboration), *Phys. Rev. D* **97**, 072013 (2018).
 - [11] A. Abdesselam *et al.* (Belle Collaboration), [arXiv: 1904.08794](https://arxiv.org/abs/1904.08794).
 - [12] Y. Amhis *et al.* (Heavy Flavor Averaging Group), *Eur. Phys. J. C* **81**, 226 (2021).
 - [13] S. Fajfer, J. F. Kamenik, and I. Nisandzic, *Phys. Rev. D* **85**, 094025 (2012).
 - [14] A. Celis *et al.*, *J. High Energy Phys.* **1301**, 054 (2013).
 - [15] A. Crivellin, G. D’Ambrosio and J. Heeck, *Phys. Rev. Lett.* **114**, 151801 (2015).
 - [16] A. Crivellin, J. Heeck, and P. Stoffer, *Phys. Rev. Lett.* **116**, 081801 (2016).
 - [17] M. Bauer and M. Neubert, *Phys. Rev. Lett.* **116**, 141802 (2016).
 - [18] M. Ablikim *et al.* (BESIII Collaboration), *Phys. Rev. Lett.* **122**, 011804 (2019).
 - [19] M. Ablikim *et al.* (BESIII Collaboration), *Eur. Phys. J. C* **76**, 369 (2016).
 - [20] M. Ablikim *et al.* (BESIII Collaboration),

Table 3. Comparison of the measured and predicted branching fractions for $D^0 \rightarrow \rho^- \mu^+ \nu_\mu$. The differences include both experimental and theoretical uncertainties for the LCSR and LFQM models; only experimental uncertainties are used for the other models.

	BESIII	LCSR [24]	LCSR [25]	LFQM [26]	CCQM [27]	CCQM [28]	χ UA [29]	RQM [30]
$\mathcal{B}_{D^0 \rightarrow \rho^- \mu^+ \nu_\mu} (\times 10^{-3})$	$1.35 \pm 0.09 \pm 0.09$	$1.73^{+0.17}_{-0.13}$	1.65 ± 0.23	1.7 ± 0.2	2.01	1.55	1.84	1.88
Difference (σ)		2.1	1.1	1.5	5.2	1.6	3.8	4.2

- Phys. Rev. Lett. **121**, 171803 (2018).
- [21] M. Ablikim *et al.* (BESIII Collaboration), Phys. Rev. D **101**, 072005 (2020).
- [22] M. Ablikim *et al.* (BESIII Collaboration), Phys. Rev. Lett **124**, 231801 (2020).
- [23] N. Isgur, D. Scora, B. Grinstein, and M. B.Wise, Phys. Rev. D **39**, 799 (1989).
- [24] Y. L. Wu, M. Zhong, and Y. B. Zuo, Int. J. Mod. Phys. A **21**, 6125 (2006).
- [25] X. Leng, X. L. Mu, Z. T. Zou, and Ying Li, Chin. Phys. C **45**, 063107 (2021).
- [26] H. Y. Cheng and X. W. Kang, Eur. Phys. J. C **77**, 587 (2017); **77**, 863(E) (2017).
- [27] N. R. Soni, M. A. Ivanov, J. G. Körner, J. N. Pandya, P. Santorelli, and C. T. Tran, Phys. Rev. D **98**, 114031 (2018).
- [28] M. A. Ivanov, J. G. Körner, J. N. Pandya, P. Santorelli, N. R. Soni, and C. T. Tran, Front. Phys. (Beijing) **14**, 64401 (2019).
- [29] T. Sekihara and E. Oset, Phys. Rev. D **92**, 054038 (2015).
- [30] R. N. Faustov, V. O. Galkin, and X. W. Kang, Phys. Rev. D **101**, 013004 (2020).
- [31] J. Koponen, C. T. H. Davies, and G. Donald (HPQCD Collaboration), arXiv:1208.6242.
- [32] J. Koponen, C. T. H. Davies, G. C. Donald, E. Follana, G. P. Lepage, H. Na, and J. Shigemitsu (HPQCD Collaboration), arXiv:1305.1462.
- [33] N. Brambilla *et al.*, Eur. Phys. J. C **74**, 2981 (2014).
- [34] J. A. Bailey *et al.* (Fermilab Lattice and MILC Collaborations), Phys. Rev. D **85**, 114502 (2012); **86**, 039904(E) (2012).
- [35] P. A. Zyla *et al.* (Particle Data Group), Prog. Theor. Exp. Phys. **2020**, 083C01 (2020).
- [36] M. Ablikim *et al.* (BESIII Collaboration), Chin. Phys. C **37**, 123001 (2013); Phys. Lett. B **753**, 629 (2016).
- [37] M. Ablikim *et al.* (BESIII Collaboration), Nucl. Instr. Method A **614**, 345 (2010).
- [38] S. Agostinelli *et al.* (GEANT4 Collaboration), Nucl. Instr. Method A **506**, 250 (2003).
- [39] S. Jadach, B. F. L. Ward, and Z. Was, Phys. Rev. D **63**, 113009 (2001); Comput. Phys. Commun. **130**, 260 (2000).
- [40] D. J. Lange, Nucl. Instrum. Meth. A **462**, 152 (2001); R. G. Ping, Chin. Phys. C **32**, 599 (2008).
- [41] J. C. Chen, G. S. Huang, X. R. Qi, D. H. Zhang, and Y. S. Zhu, Phys. Rev. D **62**, 034003 (2000).
- [42] E. Richter-Was, Phys. Lett. B **303**, 163 (1993).
- [43] M. Ablikim *et al.* (BESIII Collaboration), Phys. Rev. Lett **122**, 062001 (2019).
- [44] M. Ablikim *et al.* (BESIII Collaboration), Chin. Phys. C **40**, 113001 (2016).
- [45] M. Ablikim *et al.* (BESIII Collaboration), Phys. Rev. D **97**, 072004 (2020).
- [46] M. Ablikim *et al.* (BESIII Collaboration), Phys. Rev. Lett. **123**, 231801 (2019).
- [47] M. Ablikim *et al.* (BESIII Collaboration), Phys. Rev. D **101**, 052009 (2020).
- [48] M. Ablikim *et al.* (BESIII Collaboration), Phys. Rev. Lett **124**, 241803 (2020).
- [49] M. Ablikim *et al.* (BESIII Collaboration), Phys. Rev. Lett **125**, 141802 (2020).
- [50] M. Ablikim *et al.* (BESIII Collaboration), Phys. Rev. D **102**, 052006 (2020).
- [51] M. Ablikim *et al.* (BESIII Collaboration), Phys. Rev. D **102**, 112005 (2020).
- [52] M. Ablikim *et al.* (BESIII Collaboration), Phys. Lett. B **734**, 227 (2014).
- [53] H. Albrecht *et al.* (ARGUS Collaboration), Phys. Lett. B **241**, 278 (1990).
- [54] M. Ablikim *et al.* (BESIII Collaboration), Phys. Rev. D **89**, 051104 (2014).
- [55] M. Ablikim *et al.* (BESIII Collaboration), Phys. Rev. Lett. **123**, 211802 (2019).
- [56] M. Ablikim *et al.* (BESIII Collaboration), Phys. Rev. D **92**, 072012 (2015).
- [57] M. Ablikim *et al.* (BESIII Collaboration), Phys. Rev. D **96**, 012002 (2017).
- [58] M. Ablikim *et al.* (BESIII Collaboration), Chin. Phys. C **44**, 040001 (2020).
- [59] E. Kou *et al.* (Belle II Collaboration), PTEP **2019**, 123C01 (2019); **2020**, 029201(E) (2020).